CATIONIC SHELL CROSSLINKED NANOPARTICLES AS INTRACELLULAR DELIVERY VEHICLES FOR THE DIAGNOSIS AND TREATMENT OF ACUTE LUNG INJURY

An Honors Fellows Thesis

by

STEPHANIE FLOREZ

Submitted to the Honors Programs Office
Texas A&M University
in partial fulfillment of the requirements for the designation as

HONORS UNDERGRADUATE RESEARCH FELLOW

April 2011

Majors: Chemistry
Biomedical Science

CATIONIC SHELL CROSSLINKED NANOPARTICLES AS INTRACELLULAR DELIVERY VEHICLES FOR THE DIAGNOSIS AND TREATMENT OF ACUTE LUNG INJURY

An Honors Fellows Thesis

by

STEPHANIE FLOREZ

Submitted to the Honors Programs Office
Texas A&M University
in partial fulfillment of the requirements for the designation as

HONORS UNDERGRADUATE RESEARCH FELLOW

Approved by:

Research Advisor: Karen L. Wooley
Associate Director of the Honors Programs Office: Dave A. Louis

April 2011

Majors: Chemistry
Biomedical Science

ABSTRACT

Cationic Shell Crosslinked Nanoparticles as Intracellular Delivery Vehicles for the Diagnosis and Treatment of Acute Lung Injury. (April 2011)

Stephanie Florez
Department of Chemistry
Texas A&M University

Research Advisor: Dr. Karen L. Wooley
Departments of Chemistry and Chemical Engineering

Nanomedicine is a growing field of medicine that seeks to take advantage of nanoscale materials in order to address current challenges such as the ability to cross the epithelial mucus of the lungs to deliver treatment. This thesis focuses on the development of polymer nanomaterials known as shell crosslinked knedel-like (SCK) nanoparticles to serve as intracellular carriers of genetic material and specifically target injured cells in the lung for the treatment of acute lung injury (ALI). SCK nanoparticles are spherical in their morphology and their synthesis allows for them to possess tunable functionalities, size, and physical properties. The research presented in this work includes the synthesis of amphiphilic block copolymers that exhibit cationic character in their hydrophilic segment, in order to facilitate cell transfection in the body. The block copolymer poly(acrylamidoethylamine)$_{130}$-*block*-polysterene$_{123}$ (PAEA-*b*-PS) underwent subsequent micellization in water and crosslinking across the hydrophilic chains. The resulting SCK nanoparticles were *c.a* 75 nm in diameter and possessed cationic character. Herein, we report the physical and chemical characteristics of the block-

copolymers, micelles, and crosslinked nanoparticles. Current efforts for refining the synthetic methods in the production of SCK nanoparticles for the treatment of ALI are described.

DEDICATION

To my family:

My father, *Gonzalo Florez,*

My mother, *Shirley Malaver,*

And

My little sister, *Michelle A. Florez Malaver*

ACKNOWLEDGMENTS

I would like to thank my research advisor Dr. Karen L. Wooley, for her guidance in my research endeavors, as well as her mentorship in my future goals. My work with Dr. Wooley's laboratory has furthered my instrumental skills and knowledge in chemical synthesis, as well as empowered my self-confidence and fueled my decision in pursuing an M.D/Ph.D degree. Having Dr. Wooley as an advisor is an inspiration for any woman who wants to pursue a career in science, as well as an example for her students to keep ambitious goals and strive for excellence in all the aspects of our lives.

I want to extend my gratitude to my mentor and friend, Ph.D candidate Ritu Shrestha, for her unconditional guidance, patience, and support. Her lively personality combined with her sharp scientific mind motivated me all the way through this experience, and encouraged me to always be passionate in what I do. I am thankful with all the past and present Wooley group members, for making this group enjoyable to work with and connected like a family.

I would also like to thank the Undergraduate Research Fellows director, Dr. Dave Louis, for helping me and the other undergraduate fellows to complete our thesis and guide us through this year. I will always appreciate all the times we had a chance to talk about life and for offering me his unconditional support.

My passion for science and research started in my organic chemistry classroom, as I watched Dr. David Bergbreiter talk about this intriguing subject. I would like to thank him for he was always there helping his students and encouraging us to think beyond the books. Dr. Bergbreiter's advice has helped me make important decisions in my career such as pursuing research in the Wooley group. I will always admire his unique personality and wit that complements his incredible intelligence. I also thank my academic advisors, Dr. Elizabeth Crouch and Dr. Holly Gaede, for their guidance throughout my college career. I hold dearly my close relationship with Dr. Crouch, and would like to thank her for never doubting of my capabilities to succeed in my endeavors. I must also make a special acknowledgment of the support of Dr. Helmut Katzgraber who has constantly looked after me and helped me overcome difficult challenges in the past years.

Finally, I would like to express my deepest thanks to my friends and family who always motivated me when I most needed it. I want to thank my close friend and mentor Karen Lepley for helping me through my hardest moments, and for her unconditional love and support. My greatest gratitude goes to the most important people in my life: my father Gonzalo Florez, my mother Shirley Malaver, and my sister Michelle Florez, for their sacrifice and understanding. I thank them for teaching me the values that have allowed me to succeed, and for always reminding me of the important things in life.

NOMENCLATURE

ALI	Acute lung injury
ARDS	Acute respiratory distress syndrome
ATRP	Atomic transfer radical polymerization
cnNOS	Calcium-dependent nitric oxide synthase
cSCK	Cationic shell crosslinked (knedel-like) nanoparticle
D_h	Hydrodynamic diameter
DIPEA	N, N-Diisopropylethylamine
DLS	Dynamic light scattering
DNA	Deoxyribonucleic acid
DMF	N, N- Dimethylformamide
GPC	Gel permeation chromatography
HOBT	1-Hydroxybenzotriazole
iNOS	Inducible nitric oxide synthase
IR	Infrared spectroscopy
INF-γ	Interferon- gamma
LPS	Lipopolysaccharide
M_n	Number average molecular weight
MWCO	Molecular weight cut-off
NMR	Nuclear magnetic resonance
NO	Nitric oxide

NOS	Nitric oxide synthase
PAA	Poly(acrylic acid)
PAEA	Poly(acrylamidoethylamine)
PDI	Polydispersity index
PEG	Poly(ethylene glycol)
PEI	Polyethylenimine
PLL	Poly-L-lysine
PMDETA	N,N,N',N',N''-Pentamethyldiethylenetriamine
PNA	Peptide nucleic acid
PS/PSt	Polystyrene
P*t*BA	Poly(*tert*-butyl acrylate)
SCK	Shell crosslinked knedel-like nanoparticle
TFA	Trifluoroacetic acid
THF	Tetrahydrofuran
TNF	Tumor necrosis factor
ζ	Zeta potential

TABLE OF CONTENTS

LIST OF FIGURES

LIST OF SCHEMES

CHAPTER I

INTRODUCTION

The industrial revolution and the urbanization movement have had a major contribution to the advances in technology over the past two centuries. However, this progress runs parallel with the deterioration of the health in the world population and the increase in mortality rates particularly due to respiratory diseases[1]. Acute lung injury (ALI), stands as a major problem in industrialized countries such as the U.S, contributing to the mortality of up to 100,000 critically ill patients every year[2]. Acute lung injury is a pathological progression characterized by high-protein fluid accumulation in the lungs (pulmonary edema) and severe oxygenation impairment, which can become lethal in its most severe form known as acute respiratory distress syndrome (ARDS)[3]. ALI is caused by exposure to external agents that range from polluting gases to chemical waste, as well as many other clinical disorders. Regardless of its initiating cause, ALI is characterized by a cascade of immune cell activation and synthesis of mediating factors such and α-tumor necrosis factor (TNF), interferon- gamma (INF-γ), and nitric oxide (NO)[4]. Particularly, nitric oxide aids in the antimicrobial response of macrophages; however it been has reported that excess of NO can induce oxidative stress and lead to a septic shock and complications leading to ARDS[2]. Nitric oxide is synthesized by a family of NO synthases (NOS)[5] which can be calcium-dependent (cnNOS)[6] or cytokine-inducible (iNOS). cNOS is downregulated during ALI while iNOS expression is induced upon

---

This thesis follows the style of *Journal of the American Chemical Society*.

inflammation caused by bacteria and bacterial products such as lipopolysaccharide (LPS)[7]. Studies on iNOS show that selective inhibition of the expression of iNOS improves ALI prognosis by attenuating neutrophil accumulation into the lung[4] and furthermore that nonselective inhibition of the NOS enzymes can interfere with metabolic pathways[5, 8]. Therefore, selective antisense inhibition of iNOS has been a major focus in the treatment of ALI[9, 10, 11, 12].

In the search for a convenient antisense binding agent, properties such as stability, binding affinity to DNA and cell permeability must be taken into account[13]. Peptide nucleic acids (PNAs) stand as excellent candidates for gene delivery since they are synthetic polynucleobases that hybridize to RNA strands with higher affinity than DNA, and are resistant to removal mechanisms such as enzymatic degradation[14]. However, due to their poor cell permeability, PNAs require to be transported for cellular uptake through a carrier mechanism with higher transfection ability [15]. Although recombinant viruses make up 69% of ongoing clinical trials, their inherent mutability and poor cell-specificity make them rather limited delivery mechanisms and their behavior is difficult to predict[16]. With the rise of nanotechnology over the past twenty years, scientists have been inspired to mimic the "bottom up" approach of nature's captivating way to form molecular complexes from the self assembly of monomeric structures, adding functionality with each layer of complexity[17]. Synthetic vectors have been constructed through the assembly of smaller units that interact with each other through covalent, electrostatic, and other non-covalent interactions[18].

The most common gene delivery vectors are self assembled cationic lipids and polymers that surround DNA spontaneously and form polyplexes[19] but their low colloidal stability and low reproducibility of results called for better chemical approaches to polymer materials and methods. With the advancement in polymerization techniques, block copolymers of tunable length and compositions can be produced. Furthermore, amphiphilic block copolymers have drawn interest because of the ability to incorporate functionalities in different regions of the polymer and control in the morphology of the resulting nanostructures[20]. Amphiphilic block copolymers self assemble into micelles that achieve different morphologies from discs[21] to cylinders[22] and various other shapes[23]. To stabilize micellar structures, covalent and noncovalent crosslinkers are employed along the backbone to introduce a new class of material termed as shell crosslinked knedel-like (SCK) nanoparticles[24]. The degree of crosslinking is tunable, and it has shown to effectively gate small molecules encapsulated in the core[25], as well as provide rigidity, robustness and stability to the nanostructures against infinite dilution[26]. (Scheme 1)

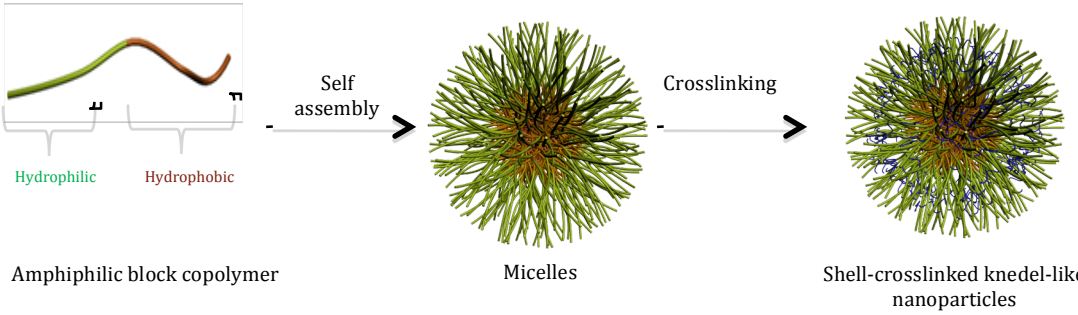

Scheme 1. General schematic representation of the construction of SCK nanoparticles

for gene delivery. Amphiphilic block copolymers self assemble into micelles, followed by crosslinking of the peripheral chains to produce well-defined SCK nanoparticles.

For the past decade, shell crosslinked knedel-like (SCK) nanoparticles have been studied as transfection agents for gene delivery [27] and labeling markers[28] due to their unique characteristics. SCKs mimic the biological structure of proteins in that they are constructed from smaller building blocks, assembled and crosslinked into a three-dimensional shape, and functionalized on their surface[24]. Parallel to advances on SCK synthesis, other groups are working on different approaches for gene delivery. Poly-L-lysine (PLL) polymers were on of the first used in gene delivery[29], but their low transfection efficiency place them as less attractive genetic carriers. However, the synthesis of PLL polymers with PEG[30], sugars[29], folate[31], and other conjugates with targeting moieties make up a large portion of current research in gene delivery, and promise to be more effective than PLL alone. In contrast to PLL, polyethylenimine (PEI) stands as one of the most effective gene-delivery up to date. PEI contains primary, secondary and tertiary amines and it is 75% protonated under physiological conditions[32]. The efficiency of PEI is due to the buffering property that its different amines provides, allowing PEI to escape endosomal uptake[33]. Despite its high efficacy for DNA delivery and interaction, PEI confers higher cytotoxicity hindering its applications in the medical field[16].

Other classes of polymers have the capacity to disrupt endosomal membrane as they become hydrophobic upon protonation. Recently, Stayton, Hoffman and co-workers synthesized pH responsive polymers with multiple functional groups that permit ligand conjugation[34]. Some of the compositions in the polymers are acrylic acids, ethylacrylic acid, butylacrylic acid, and others, but their low colloidal stability and low reproducibility of results called for better chemical approaches to polymer materials and methods. SCK nanoparticles can be engineered to disrupt endosomal membranes when their hydrophilic shell has similar composition as these polymers. Taylor, Wooley and co-workers showed in 2009 the synthesis of a cationic SCK (cSCK) particle able to escape endosomal uptake and deliver peptide nucleic acids in HeLa cells. The cationic character in the surface of the SCK was given by primary amines and showed essential for high transfection efficiency in cells as shown in comparing PLL and PEI polymers. Cationic SCKs with PEG functionalities promise have shown to decrease cytotoxicity[27], and further studies have been conducted to find a primary to tertiary amine ratio in the SCK surface that achieves the highest transfection with the lowest cytotoxicity[35]. More promising is the ability of these constructs to degrade naturally inside the cell, minimizing their cytotoxicity and waste accumulation in the spleen and liver. By introducing degradable shell, core, and crosslinkers, SCKs would be naturally metabolized in the body, reducing potential drug side-effects to its minimum[36] (Figure 1).

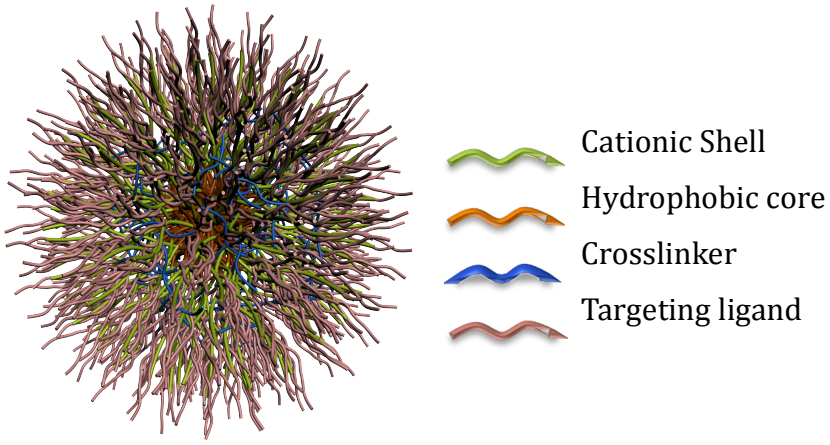

Figure 1. Functionalized cationic shell-crosslinked nanoparticle design for gene delivery and therapeutic applications

The research undertaken in this dissertation focuses on the design and construction of cSCKs for therapeutic applications in the treatment and diagnosis of ALI. Chapter II describes the methods for the synthesis block copolymer PAEA-*b*-PS, its micellization and its crosslinking to yield cationic SCK nanoparticles. In Chapter III, the experimental results are discussed along with the characterization data, to give an in-depth analysis of the physical and chemical characteristics of the structures produced. Finally, Chapter IV discusses the applications and future functionalization of the reported cSCKs, as well as current efforts to improve the synthetic methods utilized for the production of SCK nanoparticles. In summary, a strategy for fabricating cationic shell-crosslinked nanoparticles, with and without PEG functionalities is described. Furthermore, cSCKs are currently being utilized in biological assays that will measure the cell transfection efficiency of these nanomaterials; the results of these efforts will be mark a step towards the incorporation of nanotechnology in the field of medicine.

CHAPTER II

METHODS

Materials and measurements

Materials

All solvents and chemicals were purchased from Sigma-Aldrich and used without further purification, unless otherwise indicated. Homopolymer of *tert*-butyl acrylate ($P\mathit{t}BA)_{130}$ was previously synthesized by co-workers using methods previously described[37]. Styrene was filtered through an alumina plug to remove inhibitors. PEG_{2kDa} was purchased from Rapp Polymere, Germany.

Measurements

^{1}H NMR and ^{13}C NMR spectra were recorded on Inova 300 MHz or Mercury 300 MHz spectrometer interfaced to a UNIX computer using VnmrJ software. Chemical shifts were referred to the solvent resonance signals. N, N- Dimethyl formamide-based Gel Permeation Chromatography (DMF GPC) was conducted on a system equipped with a Waters Chromatography, Inc. (Milford, MA) model 1515 isocratic pump and a model 2414 differential refractometer with a three-column set of Polymer Laboratories, Inc. (Amherst, MA) Styragel columns (PL_{gel} 5μm Mixed C, 500 Å, and 10^4 Å, 300 x 7.5 mm columns) and a guard column (PL_{gel} 5μm, 50 x 7.5 mm). The system was equilibrated at 40 °C in tetrahydrofuran (THF), which served as the polymer solvent and eluent (flow rate set to 1.00 mL/min). The differential refractometer was calibrated with Polymer

Laboratories, Inc. polystyrene standards (300 to 467,000 Da). Polymer solutions were prepared at concentration *ca*. 3 mg/mL with 0.05% vol toluene as flow rate marker and an injection volume of 200 μL was used. Data was analyzed using Empower Pro software from Waters Chromatography Inc. IR spectra were recorded on an IR Prestige 21 system (Shimadzu Corp., Japan) and analyzed using IRsolution software. Dynamic light scattering (DLS) measurements were conducted using Delsa Nano C from Beckman Coulter, Inc. (Fullerton, CA) equipped with a laser diode operating at 658 nm. Size measurements were made in water (n = 1.3329, h = 0.890 cP at 25 ± 1 °C; n = 1.3293, h = 0.547 cP at 50 ± 1 °C; n = 1.3255, h = 0.404 cP at 70 ± 1 °C). Scattered light was detected at 15° angle and analyzed using a log correlator over 70 accumulations for a 0.5 mL of sample in a glass size cell (0.9 mL capacity). The photomultiplier aperture and the attenuator were automatically adjusted to obtain a photon counting rate of *ca*. 10 kcps. The calculation of the particle size distribution and distribution averages was performed using CONTIN particle size distribution analysis routines. Prior to analysis, the samples were filtered through a 0.45 μM Whatman Nylon membrane filter (Whatman Inc.). The samples in the glass size cell were equilibrated at the desired temperature for 60 minutes before measurements were made. The peak average of histograms from intensity, volume or number distributions out of 70 accumulations was reported as the average diameter of the particles.

Methods

Poly(t-butyl acrylate)-block-polystyrene ($PtBA_{130}$-b-PS_{123})

Poly(*tert*-butyl acrylate) P*t*BA (2.0 g, 0.12 mmol) was added to a flame- dried 50 mL Schlenk flask equipped with a magnetic stir bar. Styrene (1.85 g, 17.8 mmol), CuBr (34 mg, 0.24 mmol), and anisole were added and stirred for homogenous mixing and the flask was sealed with a rubber septum. After 10 min, the reaction flask was freeze-pump-thawed 3 times, after which the flask was allowed to return to room temperature. PMDETA (4.0 mg, 37 μmol) was added and the reaction mixture was degassed by another freeze-pump-thaw cycle. The flask was then immersed into a pre-heated oil bath at 82 °C to start the polymerization. The polymerization was monitored by analyzing aliquots collected at pre-determined times by ^{1}H NMR spectroscopy. The expected monomer conversion was reached after 2 h, and the reaction was quenched by immersion in liquid nitrogen. The reaction was precipitated in 2 L of cold methanol twice. The precipitants were collected, dissolved in CH_2Cl_2 and dried with magnesium sulfate. Then reaction was rotorvapped to obtain a white polymer. M_n^{NMR}= 29.7 kDa; M_n^{GPC}= 40.4 kDa. IR (cm^{-1}): 3001, 2924, 1728, 1450, 1365, 1150. ^{1}H NMR (300 MHz , $CDCl_3$): δ 1.36 (m, C***H*****$_3$**CH_2–), 1.85 (br, –CHC***H*****$_2$**– of the polymer backbone, alkyl chain of initiator, and HOOCC(C***H*****$_3$**$)_2$–), 1.97 (br, C***H*****$_3$**C), 2.13–2.38 (br, –C***H***CH_2– of the polymer backbone), 6.32–7.21 (br, *Ar–H*) ppm.

Poly(acrylic acid)-block-polystyrene (PAA_{130}-b-PS_{123})

To a flame-dried 100 mL round bottom flask equipped with a stir bar, P*t*BA_{130}-*b*-PS_{123} (4.8 g, 0.30 mmol) was dissolved in 10mL CH_2Cl_2. 15 mL of TFA were added to the solution and the reaction mixture was stirred overnight, after which the solvent was removed under vacuum. The crude product was dissolved in THF and transferred to a presoaked dialysis tubing (MWCO ca. 6000–8000 Da), and dialyzed against nanopure H_2O for 4 days, yielding polymer PAA_{130}-*b*-PS_{123}. M_n^{NMR}= 22.2 kDa. IR (cm^{-1}): 3000-2500 broad, 3032, 2916, 1705, 1450, 1242, 1172. ^1H NMR (500 MHz, $(CD_3)_2SO$): δ 0.85 (m, C***H*****$_3$**CH_2–), 1.21–1.87 (br, –CHC***H*****$_2$**– of the polymer backbone, alkyl chain of initiator, and HOOCC(C***H*****$_3$**$)_2$–), 2.10–2.41 (br, –C***H***CH_2– of the polymer backbone), 6.31–7.27 (br, *Ar*–***H***) ppm.

Poly(acrylamidoethylamine)$(Boc)_{130}$-block-polystyrene$_{123}$ ($PAEA(Boc)_{130}$-b-PS_{123})

PAA_{130}-*b*-PS_{123} (150 mg, 6.75 μmol, 0.877 mmol carboxylic acid groups) was dissolved in DMF (5.0 mL) and stirred for 1 h. After dissolving the reaction mixture, a 2.0 mL DMF solution containing HOBT (155 mg, 1.14 mmol) and HBTU (433 mg, 1.14 mmol) was added. After 30 min, N-Boc-ethylenediamine (211 mg, 1.31 mmol) and diisopropylethylamine (DIPEA) (198 μL, 1.14 mmol) were added. The reaction mixture stirred overnight, was diluted in 10 mL of DMF, transferred to pre-soaked dialysis tubing (MWCO ca. 6000–8000 Da), and was dialyzed against 150 mm NaCl solution for 2 days, followed by dialysis in nanopure water (18.0 MΩ cm) for 5 days. Precipitation occurred shortly after the dialysis began. After the dialysis period, the polymer was

lyophilized yielding polymer PAEA(Boc)$_{130}$-b-PS$_{123}$. M_n^{NMR}= 32.1 kDa; M_n^{GPC}= 8.5 kDa. IR (cm^{-1}): 3456-3224, 2977, 2916, 1689, 1658, 1549, 1450, 1365, 1257, 1165. ^{1}H NMR (500 MHz, $(CD_3)_2SO$): 1.05–2.52 (br, Boc protons and polymer backbone protons), 2.85–3.65 (br, NHC***H***$_2$C***H***$_2$NH$_2$), 5.60–6.33 (br, N***H***), 6.35–6.80 and 6.88–7.40 (br, Ar***H***) ppm. ^{13}C NMR (75 MHz, CD_2Cl_2): 27.6 (br), 38.8–40.0 (multiple overlapping br), 77.6 (br), 126.2 (br), 128.4 (br), 145.9 (br), 157.1 (br), 176.4 (br) ppm.

Poly(acrylamidoethylamine)$_{130}$-block-polystyrene$_{123}$ (PAEA$_{130}$-b-PS$_{123}$)

PAEA(Boc)$_{130}$-*b*-PS$_{123}$ (100 mg, 4.47 μmol) was dissolved in TFA (4 mL) and stirred for 2 h. The solution was then rotorvapped and transferred to a presoaked dialysis tubing (MWCO ca. 6000–8000 Da), and dialyzed against nanopure H_2O for 4 days, to remove all of the impurities. The solution was lyophilized to yield polymer PAEA$_{130}$-b-PS$_{123}$. M_n^{NMR}: 25.1 kDa. IR (cm^{-1}): 3700–2600, 1681, 1556, 1434, 1204, 1180, 1134, 844. ^{1}H NMR (500 MHz, $(CD_3)_2SO$): 0.95–2.24 (br, polymer backbone protons), 3.00–3.47 (br, NHC***H***$_2$C***H***$_2$NH$_2$), 6.20–6.80 and 6.81–7.33 (br, Ar***H***), 7.82–8.49 (br, N***H***) ppm. ^{13}C NMR (75 MHz, DMSO-d_6): 31.3, 32.5–45.0 (multiple overlapping br), 125.7 (br), 127.4 (br), 128.0 (br), 145.7 (br), 175.0 (br) ppm.

Synthesis of crosslinker, 14-oxo-7,10-dioxa-4,13-diazaheptadecane-1,17-dioic acid

1, 2-Bis(2-aminoethoxy)ethane (100 mg, 0.675 mmol) was dissolved in DMF (1 mL), to which a DMF solution (1.35 mL) containing succinic anhydride (135 mg, 1.35 mmol) and DIPEA (235 μL, 1.35 mmol) was added slowly. The reaction mixture was stirred

overnight and then the product was precipitated into pure diethyl ether (4×), and collected by centrifugation and decanting of the supernatant, and was dried in vacuo overnight (yield: 132 mg, 76%). IR (cm^{-1}): 3600–2300, 2928, 1716, 1651, 1557, 1418, 1201, 1134. ^{1}H NMR (300 MHz, DMSO-d6): 2.35 (t, J = 6 Hz, 4H, $CH_2C\mathbf{H_2}CONH$), 2.41 (t, J = 6 Hz, 4H, $C\mathbf{H_2}CH_2CONH$), 3.20 (t, J = 5.4 Hz, 4H, $NHC\mathbf{H_2}CH_2O$), 3.40 (t, J = 5.4 Hz, 4H, $NHCH_2C\mathbf{H_2}O$), 3.52 (s, 4H, $OC\mathbf{H_2}C\mathbf{H_2}O$) ppm. 13C NMR (75 MHz, DMSO-d6): 29.8, 30.5, 39.3, 70.1, 70.5, 171.9, 174.8 ppm.

Micellization of block copolymers

$PAEA_{130}$-b-PS_{123} (21 mg, 0.82 μmol) was dissolved in 20 mL dimethylsulfoxide (DMSO) and stirred for 2 h. The solution was then transferred to a pre-soaked dialysis tube (8000 Da MWCO) and dialyzed against nanopure water (18.0 MΩ cm) to remove organic solvent. After 4 days of dialysis, a clear solution (59 mL) containing the micelle precursors for the cSCKs was obtained. DLS: $(D_h)_{int}$ = 153 ± 55 nm, $(D_h)_{vol}$ = 96 ± 37 nm, $(D_h)_{num}$ = 75 ± 20 nm. ζ potential: 40 ± 3 mV.

Crosslinking of micelles to afford cationic SCKs

The diacid crosslinker (0.46 mg, 1.3 μmol) was activated by mixing with 2.2 equiv. of HOBt/HBTU (0.39 mg/1.10 mg, 1:1, mol:mol) in DMF (410 μL) and allowed to stir for 1 h. The micelle solution pH was adjusted to 8.0, using 1.0 m aqueous sodium carbonate, and submerged in an ice bath at 0 °C. The stirred solution with activated crosslinker was

added dropwise with stirring to the micelle solution. The reaction mixture was allowed to stir overnight.

CHAPTER III

RESULTS

Block copolymers composed of segments of PAEA and PS were chosen to be the building blocks in the preparation of well-defined functionalized cationic shell crosslinked nanoparticles for the treatment of acute lung injury. The synthetic avenue chosen to achieve the final block copolymers started with the chain extension of previously synthesized homopolymer of P*t*BA by sequential atomic transfer radical polymerization (ATRP) (Scheme 2). Using PMDETA/CuBr as a catalyst, the reaction underwent completion after two hours. The oxidation of Cu(I) to Cu(II) can decrease the reaction efficiency, therefore P*t*BA and CuBr were added to the flask and put under a nitrogen atmosphere prior to PMDETA addition. The reaction was monitored by ^{1}H NMR, where the presence of the aromatic hydrogen atoms in the product served to quantify the number of styrene units (123 u.) present in the resulting block copolymer. GPC showed a decrease in the retention time, allowing us to confirm that a chain lengthening process occurred (Figure 2). The polydispersities of P*t*BA$_{130}$ and P*t*BA$_{130}$-*b*-PS$_{123}$ were narrow being 1.05 and 1.09 respectively, characteristic of ATRP polymerization.

Cleavage of the *tert*-butyl ester groups was then performed *via* reaction with anhydrous TFA after dissolving the polymer in dichloromethane at room temperature, affording amphiphilic block copolymer PAA$_{130}$-*b*-PS$_{123}$. Deprotection was confirmed by ^{1}H NMR

with the disappearance of the Boc protons at 1.3 ppm that indicated presence of *tert*-butyl functionalities. Furthermore, IR spectra showed a broad peak in the 3000-2500 cm^{-1} region, indicating the characteristic stretch of a carboxylic acid O-H (Figure 3).

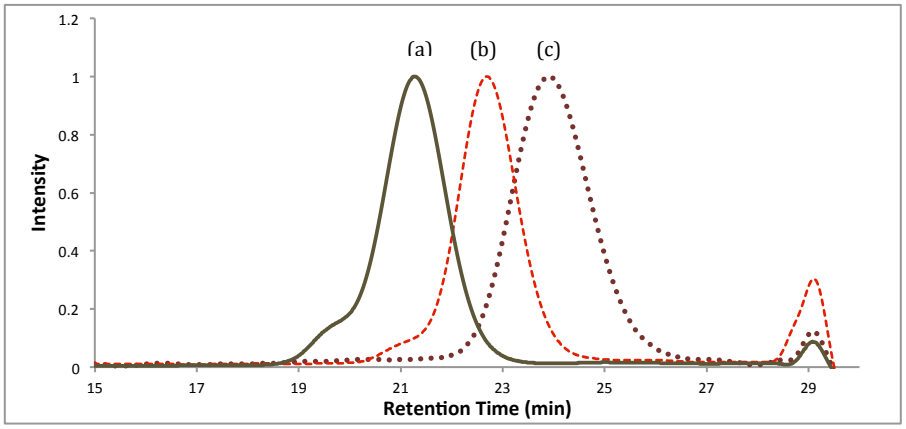

Figure 2. Composite of GPC data for polymers PAEA(Boc)-*b*-PS (a), P*t*BA-*b*-PS (b), and P*t*BA (c). This graph illustrates the growth of the polymer chain as the retention time in the column decreases

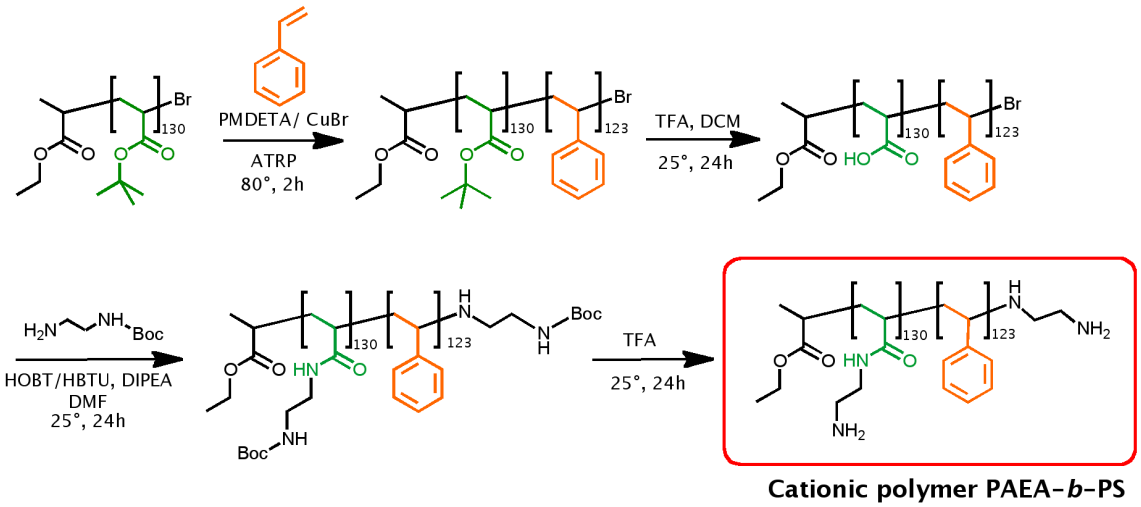

Scheme 2. Synthetic route for the formation of cationic block copolymer PAEA-*b*-PS

Previous studies in cell transfection and gene delivery have shown that cationic charges on delivery vectors promote cell uptake and endosomal release by the proton-sponge effect [38, 39]. To achieve a cationic charge, the carboxylic acid functionalities were allowed to react with mono-Boc-protected ethylenediamine *via* amidation chemistry. Conversion into the Boc-protected amine polymer was confirmed by ^{13}C NMR where the Boc-carbamate and the polymer amide carbons were seen at 176.4 and 157.1 respectively. GPC showed an increase in molecular weight compared to P*t*BA$_{130}$-*b*-PS$_{123}$ as expected (figure 2), and a moderate polydispersity of 1.25. After subsequent deprotection using TFA, the resulting polymer PAEA$_{130}$-*b*-PS$_{123}$ was analyzed by ^{1}H NMR where the loss of the Boc protons confirmed deprotection. Both the amidation reaction and deprotection were further analyzed by IR, where the mono-Boc-protected secondary amine showed a weak band in in the 3300-3000 cm^{-1} region, compared to the deprotected primary amine that had two characteristic bands between 3400-3100 cm^{-1} as well as NH bend at 1550 cm^{-1} unique to primary amines.

PAEA$_{130}$-*b*-PS$_{123}$ was then dissolved in DMSO and underwent micellization by direct dialysis in nanopure water. The micelle concentration was measured to be 0.70 mg/mL and gave a clear solution with no signs of precipitation. Micelles were analyzed by DLS which showed a hydrodynamic diameter by number average of 75 ± 20 nm and a zeta-potential of 40 ± 3 mV, confirming their cationic character. The final crosslinking step required first the preparation of the diacid crosslinker 14-oxo-7,10-dioxa-4,13-diazaheptadecane-1,17-dioic acid, which was chosen for its effective reactivity with

primary amines when activated. Activation of the crosslinker was performed with 2.2 eq. of HOBT/HBTU (1:1 mol) in DMF, to achieve crosslinking of 5% of the peripheral amines of the micelles.

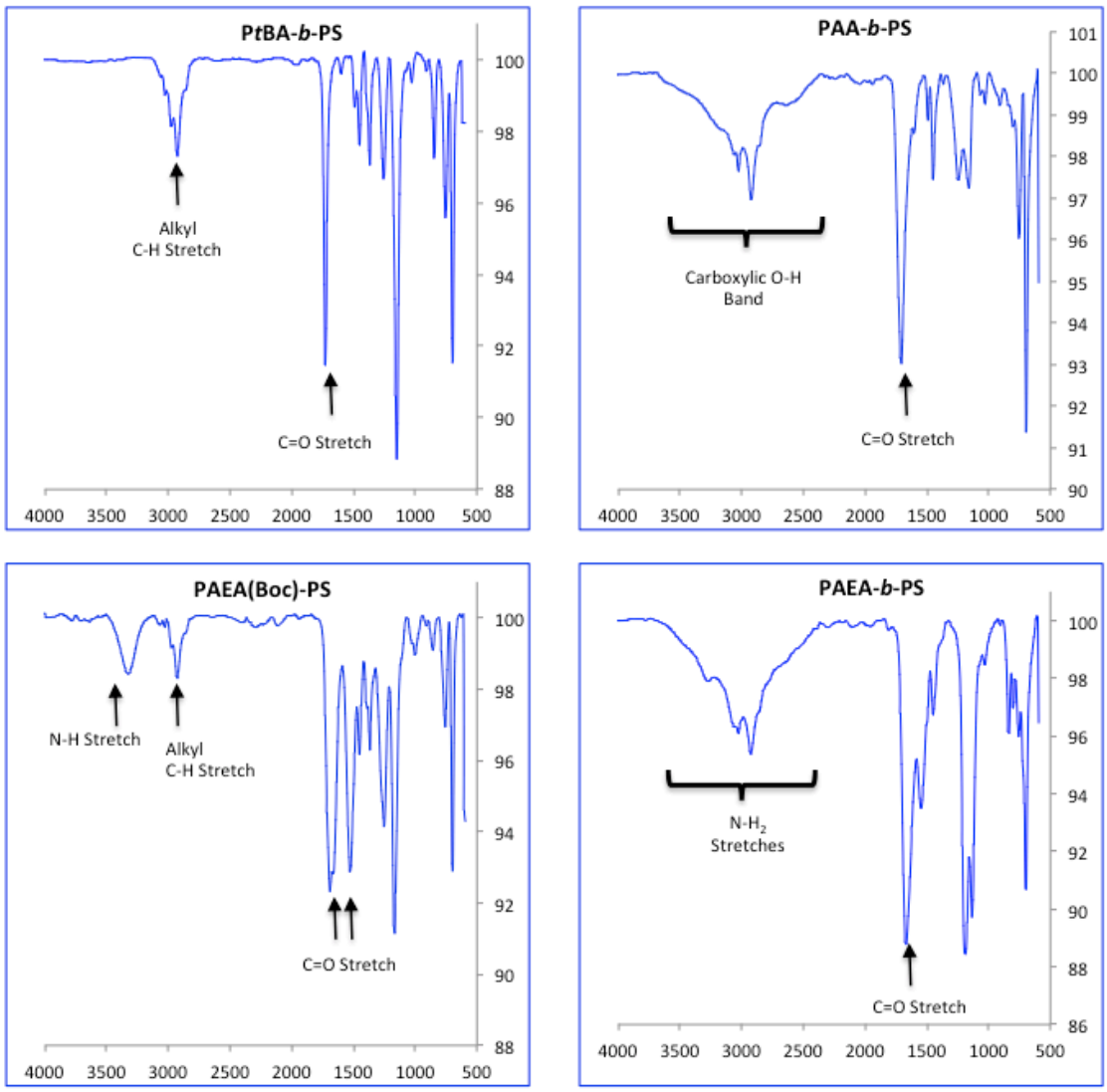

Figure 3. Infrared spectroscopy data shows the transformation of the functional groups in the hydrophilic domain during pre-assembly modifications of the block copolymer

The crosslinker was added dropwise to the micelle solution with gentle stirring. Initially, a clear solution was observed however a small amount of precipitation was seen after 10 minutes of stirring. The experiment was repeated several times where factors such as solvent, type of base and pH were adjusted one at a time, yet the micelles did not undergo crosslinking and precipitated after each attempt. We hypothesize that after the first deprotection reaction that cleaved the *tert*-butyl from P*t*BA was incomplete, leaving behind *tert*-butyl groups that did not undergo amidation, and after the second deprotection converted them into carboxylic acids. During crosslinking, carboxylic acids and amines might have undergone intramolecular crosslinking processes that caused micelle disruption and macroscopic precipitation. Therefore, it is key to ensure that the first deprotection step is carried through completely in order to ensure efficient crosslinking and SCK assembly.

CHAPTER IV

SUMMARY AND CONCLUSIONS

In this work, we have used controlled radical polymerization to construct a block copolymer with amphiphilic characteristics and controlled chain length. Modifications to the hydrophilic segment by amidation chemistry yielded block copolymer PAEA-*b*-PS. These block copolymers underwent micellization under aqueous conditions, and further crosslinking to give cationic shell crosslinked nanoparticles. Physico-chemical analysis of the structures and intermediates confirmed the cationic charge, spherical structure and diameter of the nanoconstructs. Although crosslinking of the micelles did not go to completion, it allowed us to define the most important steps in the synthetic process. Complete cleveage of the *tert*-butyl groups in P*t*BA is a key step in the synthesis of the final block-copolymer. Allowing the deprotection reaction run for a longer time, and monitoring with NMR until all tert-butyl protons are removed will be part of future protocols.

Well-defined cationic SCKs can serve as potential gene delivery vehicles to cells with overexpressed iNOS during ALI. We expect that the cationic charge in the nanoparticles will give them higher transfection efficiency through the proton-sponge effect. This phenomenom occurs when the nanoparticles are endocytosed in vesicles inside the cell and engulfed by lysosomes. The primary amines of the SCKs will sequester the protons inside the lysosome's acidic environment, causing the swelling of the lysosome and

subsequent rupture. This allows for the nanoparticles to be dispersed in the cytoplasm and efficiently transfect cells[40]. Furthermore, the size of the nanoparticles is small enough to cross the epithelial and mucosal barrier[41]. By conjugating cSCKs to nucleic bases complementary to iNOS, antisense binding can be achieved in order to prevent further iNOS translation as well as down-regulation of the transcription of these genes. Overall, it is expected that the inhibition due to the SCK-mRNA complex will decrease the toxic levels of nitric oxide, reduce inflammation, and alleviate the symptoms of acute lung injury.

Currently, studies regarding the re-dispersion of the SCKs upon exposure to different media are being studied, in order to understand the behavior of the nanoparticles in a variety of conditions. Moreover, the incorporation of biodegradable segments in the core, periphery, and crosslinking moieties would allow the SCK to have minimal toxicity inside the body, breaking down the nanospheres into small monomeric units that the body can recycle or metabolize. This is a promising stepping-stone in the incorporation of cSCKs as treatments in acute lung injury, and a variety of other conditions that require selective toxicity. Beyond their applicational purpose, studies using SCKs as transfection agents, will give insight into the natural events inside the cell that are essential to understand for the refinement of these technologies; mechanisms such as the proton-sponge effect, as well as the inflammatory processes that occur inside the lung are among the list.

As this thesis suggests, the field of nanomedicine is rapidly growing and becoming a potentially important tool in drug delivery. As technology pushes forward the construction of nanomaterials with a broad range of applications, so does our understanding in the behavior of the molecular world around us. Therefore, nanoscience and nanomedicine not only promises a revolutionary approach to solve current challenges, but it mediates further understanding and incites the creation of new ideas that can be undertaken by future generations.

REFERENCES

1. Sullivan, J., *Epidemiology* **2005,** *16* (1), 41.
2. Mehta, S., *Vascul. Pharmacol.* **2005,** *43* (6), 390-403.
3. Orfanos, S. E.; Mavrommati, I.; Korovesi, I.; Roussos, C., Pulmonary endothelium in acute lung injury: from basic science to the critically ill. In *Applied Physiology in Intensive Care Medicine*, Hedenstierna, G.; Mancebo, J.; Brochard, L.; Pinsky, M. R., Eds. Springer, Berlin Heidelberg: 2009; pp 215-227.
4. Numata, M.; Suzuki, S.; Miyazawa, N.; Miyashita, A.; Nagashima, Y.; Inoue, S.; Kaneko, T.; Okubo, T., *J. Immunol.* **1998,** *160* (6), 3031-3037.
5. Nathan, C., *FASEB J.* **1992,** *6* (12), 3051-3064.
6. Scott, J. A.; McCormack, D. G., *Can. J. Physiol. Pharmacol.* **1999,** *77* (2), 89-95.
7. Ermert, M.; Ruppert, C.; Günther, A.; Duncker, H.-R.; Seeger, W.; Ermert, L., *Lab. Invest.* **2002,** *82* (4), 425-441.
8. Nathan, C. F., *J. Clin. Invest.* **1987,** *79* (2), 319-326.
9. Xiu-li, W.; Wen-jun, C.; Hui-hua, D.; Su-ping, H.; shi-long, F., *Mol. Immunol.* **2009,** *46* (11-12), 2413-2418.
10. Harkin, D. W.; Rubin, B. B.; Romaschin, A.; Lindsay, T. F., *J. Surg. Res.* **2004,** *120* (2), 230-241.
11. Hong, C. H.; Hur, S. K.; Oh, O. J.; Kim, S. S.; Nam, K. A.; Lee, S. K., *J. Ethnopharmacol.* **2002,** *83* (1-2), 153-159.
12. Lieb, K.; Engels, S.; Fiebich, B. L., *Neurochem. Int.* **2003,** *42* (2), 131-137.

13. Milligan, J. F.; Matteucci, M. D.; Martin, J. C., *J. Med. Chem.* **1993,** *36* (14), 1923-1937.

14. Fang, H.; Zhang, K.; Shen, G.; Wooley, K. L.; Taylor, J.-S. A., *Mol. Pharm.* **2009,** *6* (2), 615-626.

15. Giovine, M.; Gasparini, A.; Scarfì, S.; Damonte, G.; Sturla, L.; Millo, E.; Tonetti, M.; Benatti, U., *FEBS Lett.* **1998,** *426* (1), 33-36.

16. Pack, D. W.; Hoffman, A. S.; Pun, S.; Stayton, P. S., *Nat. Rev. Drug. Discov.* **2005,** *4* (7), 581-593.

17. Fletterick, R. J., *Proteins* **1992,** *12* (2), 200-200.

18. Whitesides, G. M.; Grzybowski, B., *Science.* **2002,** *295* (5564), 2418-2421.

19. Zabner, J., *Adv. Drug Del. Rev.* **1997,** *27* (1), 17-28.

20. Dawkins, J., *Polym. Int.* **2004,** *53* (2), 232-232.

21. Li, Z.; Chen, Z.; Cui, H.; Hales, K.; Qi, K.; Wooley, K. L.; Pochan, D. J., *Langmuir.* **2005,** *21* (16), 7533-7539.

22. Wang, X.; Guerin, G.; Wang, H.; Wang, Y.; Manners, I.; Winnik, M. A., *Science.* **2007,** *317* (5838), 644-647.

23. Wang, H., *J. Am. Chem. Soc.* **2007,** *129* (43), 12924-12925.

24. Thurmond, K. B.; Kowalewski, T.; Wooley, K. L., *J. Am. Chem. Soc.* **1996,** *118* (30), 7239-7240.

25. Nystrom, A. M.; Xu, Z.; Xu, J.; Taylor, S.; Nittis, T.; Stewart, S. A.; Leonard, J.; Wooley, K. L., *Chem. Commun.* **2008,** (30), 3579-3581.

26. Wooley, K. L., *J. Polym. Sci., Part A: Polym. Chem.* **2000,** *38* (9), 1397-1407.

27. Zhang, K.; Fang, H.; Shen, G.; Taylor, J.-S. A.; Wooley, K. L., *Proc. Am.Thorac. Soc.* **2009,** *6* (5), 450-457.

28. Sun, G.; Xu, J.; Hagooly, A.; Rossin, R.; Li, Z.; Moore, D. A.; Hawker, C. J.; Welch, M. J.; Wooley, K. L., *Adv. Mater.* **2007,** *19* (20), 3157-3162.

29. Wu, G. Y.; Wu, C. H., *J. Biol. Chem.* **1987,** *262* (10), 4429-4432.

30. Nishikawa, M., *J. Pharmacol. Exp. Ther.* **1998,** *287* (1), 408-415.

31. Choi, Y. H.; Liu, F.; Kim, J.-S.; Choi, Y. K.; Jong Sang, P.; Kim, S. W., *J. Controlled Release* **1998,** *54* (1), 39-48.

32. Garnett, M. C., *Crit. Rev. Ther. Drug. Carrier. Syst.* **1999,** *16* (2), 147-207.

33. Boussif, O.; Lezoualc'h, F.; Zanta, M. A.; Mergny, M. D.; Scherman, D.; Demeneix, B.; Behr, J. P., *Proc. Natl. Acad. Sci. U. S. A.* **1995,** *92* (16), 7297-7301.

34. Murthy, N.; Chang, I.; Stayton, P.; Hoffman, A., *Macromol. Symp.* **2001,** *172* (1), 49-56.

35. Zhang, K.; Fang, H.; Wang, Z.; Li, Z.; Taylor, J.-S. A.; Wooley, K. L., *Biomaterials.* **2010,** *31* (7), 1805-1813.

36. Iha, R. K.; van Horn, B. A.; Wooley, K. L., *J. Polym. Sci., Part A: Polym. Chem.* **2010,** *48* (16), 3553-3563.

37. Nyström, A. M.; Wooley, K. L., *Tetrahedron.* **2008,** *64* (36), 8543-8552.

38. Lee, Y.; Miyata, K.; Oba, M.; Ishii, T.; Fukushima, S.; Han, M.; Koyama, H.; Nishiyama, N.; Kataoka, K., *Angew. Chem.* **2008,** *120* (28), 5241-5244.

39. Zhang, K.; Fang, H.; Wang, Z.; Taylor, J.-S. A.; Wooley, K. L., *Biomaterials.* **2009,** *30* (5), 968-977.

40. Nel, A. E.; Madler, L.; Velegol, D.; Xia, T.; Hoek, E. M. V.; Somasundaran, P.; Klaessig, F.; Castranova, V.; Thompson, M., *Nat. Mater.* **2009,** *8* (7), 543-557.

41. Rytting, E.; Nguyen, J.; Wang, X.; Kissel, T., *Expert Opinion on Drug Delivery* **2008,** *5* (6), 629-639.

CONTACT INFORMATION

Name:	Stephanie Florez
Professional Address:	c/o Dr. Karen Wooley Department of Chemistry RM 4126 Texas A&M University College Station, TX 77843
Email Address:	florezstephanie@tamu.edu
Education:	B.S., Chemistry and Biomedical Science Texas A&M University, May 2013 Magna Cum Laude Honors Undergraduate Research Fellow Phi Epsilon Sigma